Source Complexity of the 2016, M_w 6.2, August 24th Amatrice Earthquake from Non Linear Inversion of Strong Motion Data

2016, September 8

Antonella Cirella, Alessio Piatanesi

antonella.cirella@ingv.it

Cite as: *Source Complexity of the 2016 Amatrice Earthquake from Non Linear Inversion of Strong Motion Data: Preliminary Results;*
DOI:10.5281/zenodo.153821

Istituto Nazionale di Geofisica e Vulcanologia
Department of Seismology and Tectonophysics
Via di Vigna Murata 605,
00143 Rome,
Italy

Fault Model

The 2016 Amatrice earthquake occurred on August 24 at 01:36 UTC, 13.238E, 42.704N, 8.1 km depth.
The focal mechanism, estimated by moment tensor analysis, reveals the following fault parameters (http://cnt.rm.ingv.it/~earthquake):

-TDMT: (P1 strike: 156, dip: 50, rake: -85; P2 strike: 328, dip: 41, rake: -96)
In this first inversion attempt we assume the TDMT focal mechanism and the following fault plane model:

- along strike dimension: 30 km, spatial discretization: 2.5 km;
- along dip dimension: 17.5 km, spatial discretization: 2.5 km;
- nucleation point (hypocenter): Lon 13.238 E; Lat 42.704 N, 8.1 km depth;
- depth of the upper border of the fault plane: 0.5 km;

Inversion methodology

We used a two-stage nonlinear inversion method (*Piatanesi et al.* 2007; *Cirella et al.*, 2008); this technique is able to jointly invert strong ground motions records and geodetic data. The extended fault is divided into subfaults with model parameters assigned at the corners; the value of every parameter is not constant inside the subfault but it spatially varies through a bilinear interpolation of the nodal values. At each point on the fault the rupture model is described by four model parameters: rise time, rupture time, peak slip velocity and rake angle. Each point on the fault can slip only once (single window approach) and the source time function can be selected among different analytical forms. The nonlinear global inversion consists of two stages. In the first stage an heat-bath simulated annealing algorithm builds up the model ensemble. In the second stage the algorithm performs a statistical analysis of the ensemble providing us the best-fitting model, the average model and the associated standard deviation.

Data

We used strong motion data of 22 stations (Figure1) operated by RAN (Rete Accelerometrica Nazionale,) and by INGV. Original acceleration recordings are integrated to obtain ground velocity time histories. The resulting velocity waveforms are band-pass filtered between 0.02 and 0.5 Hz using a two-pole and two-pass Butterworth filter. We invert 40 seconds of each waveform, including body and surface waves. The Green's functons are computed by assuming the CIA crustal model proposed by Hermann et al. 2011.

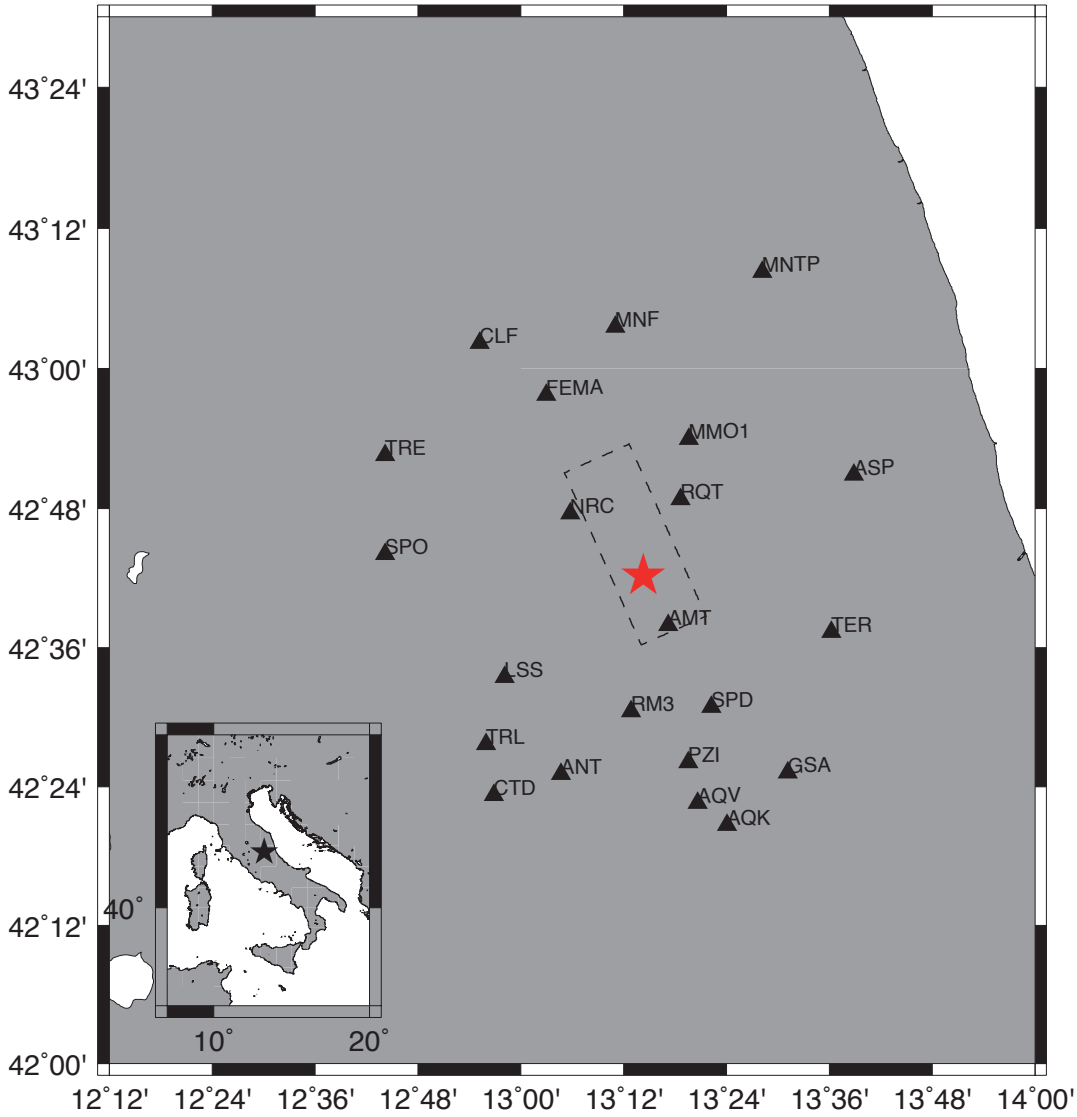

Figure1. Map of the fault geometry of the 2016 Amatrice earthquake. The black box represents the surface projection of the fault plane adopted in this study. Black triangles represent INGV and RAN strong motion stations. Red star is the position of the epicentre.

Results

All kinematic parameters (peak slip velocity, rise time, rupture time and slip angle) are simultaneously inverted by adopting the following variability intervals: peak slip velocity values can range between 0 and 3.5 m/s at 0.25 m/s interval; the rise time between 0.75 and 3 sec at 0.25 sec interval and the rake angle in the range of -85° ± 30° in steps of 10°. The rupture time at each grid node is constrained by the arrival time from the hypocenter of a rupture front having a speed comprised between 1.4 and 4 km/s. Figure 2a) shows the obtained rupture model in terms of slip, rise time, peak slip velocity, rake angle distributions on the fault; and the propagating rupture front. This model is obtained by averaging a subset of the model ensemble, corresponding to those models having a cost function exceeding by 5% the minimum value of the cost function reached during the inversion. The upper panel in Figure 2a) displays the final slip distribution; middle and lower panels show the rise time

and the peak slip velocity distributions on the fault plane, respectively. The upper panel also shows the rupture fronts and the bottom panel the slip direction at each grid node. Figure2b) displays the comparison between recorded (blue) and predicted (red) waveforms. The seismic moment of the retrieved model is M_o = 2.5 x 10^{18} Nm.

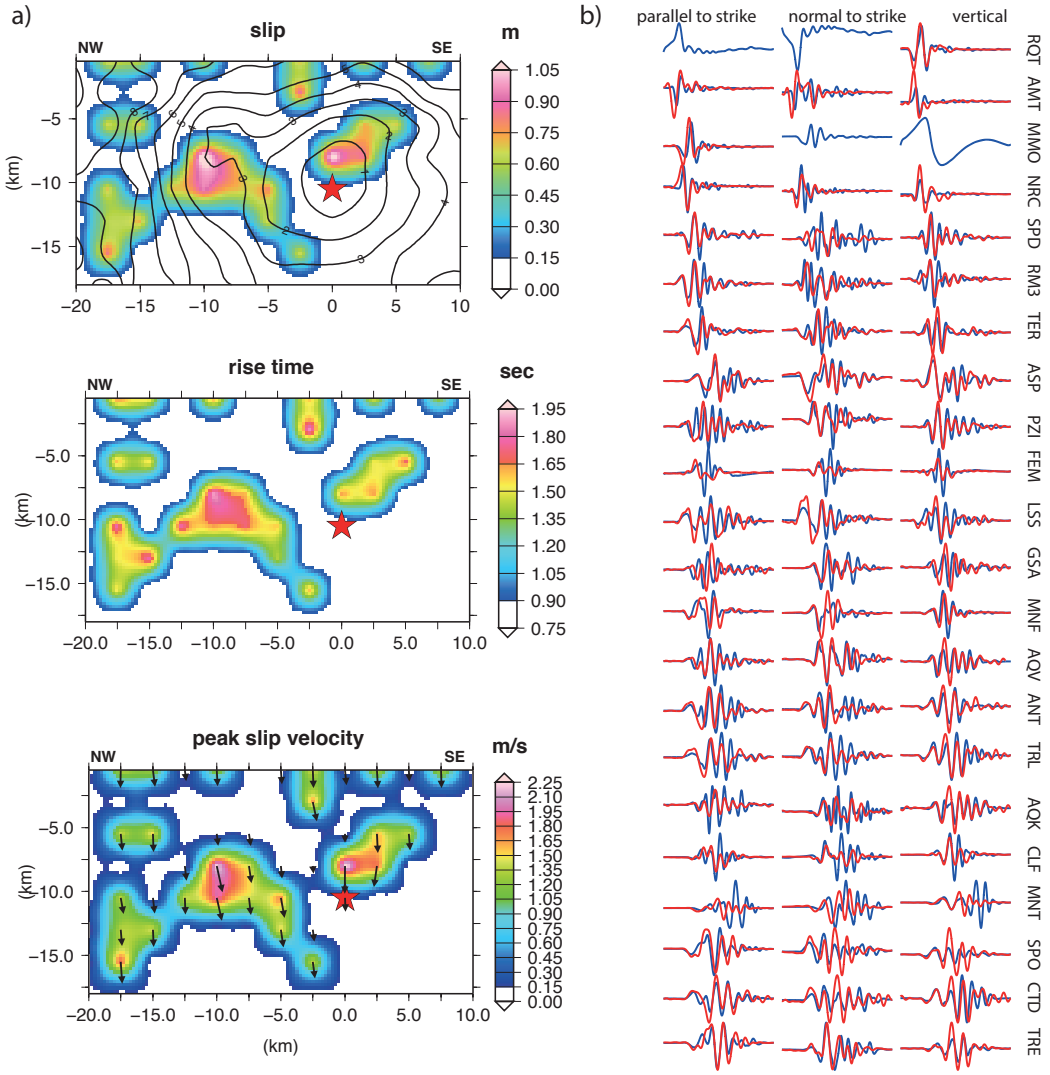

Figure 2. a) Inverted rupture model (average model from ensemble inference). Upper, middle and lower panels show the total slip, the rise time and the peak slip velocity distributions, respectively. Rupture time shown by black contour lines (in seconds) in the upper panel; black arrows displayed in bottom plot represent the slip vector. b) Comparison between recorded (blue) and predicted (red) waveforms.

In order to investigate the complexity of the obtained rupture model and its heterogeneities we have plotted in Figure 3, by following the work of Cirella et al. (2012), both the local rupture velocity (panel a)) imaged from the retrieved rupture times and the associated distribution on the fault plane of the rupture mode coefficient (panel b). According to Pulido & Dalguer (2009), rup=0 corresponds to a Mode II (in plane) crack propagation, while rup = 1 to a Mode III (anti-plane). We have to be carefully to investigate these features only on the fault portion that slipped during the earthquake (identified by the slip contour in Figure3 (white and black lines, in panel a) and b), respectively).

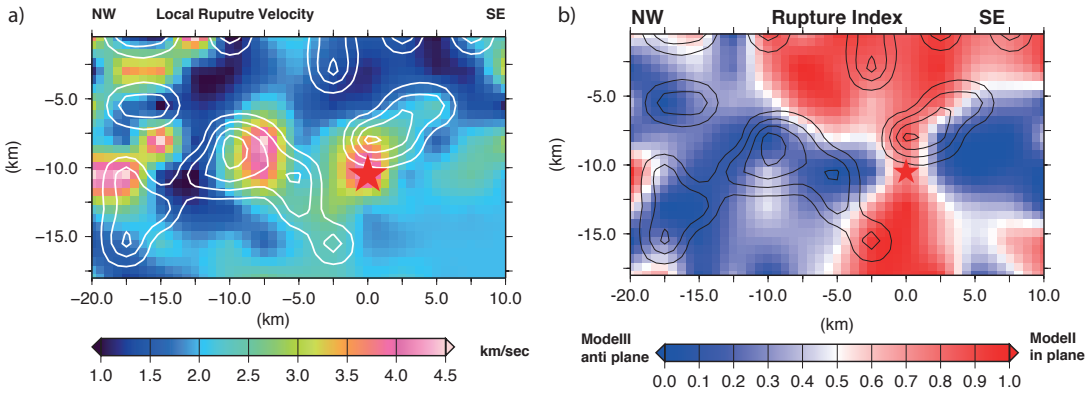

Figure 3. (a) Local rupture velocity distribution on the fault plane for the 2016 Amatrice main shock overlapped by the slip contour (white line, in metres). (b) Rupture index displaying the rupture mode across the fault plane for the 2016 Amatrice earthquake, overlapped by the slip contour (black line, in metres). Values towards 1 correspond to a pure Mode II (in-plane) rupture, values towards 0 to a pure Mode III (anti-plane) rupture. Values in between correspond to a mixed rupture mode.

Figure4 shows the retrieved rupture model projected on the Earth surface with villages up to 20km distant from the nucleation. Colors on the fault plane indicate the slip distribution; black contours represent the position of the propagating rupture at 1 s interval. Violet line displays the location of the observed surface breakages (provided by S. Gori & E. Falcucci- EMERGEO).

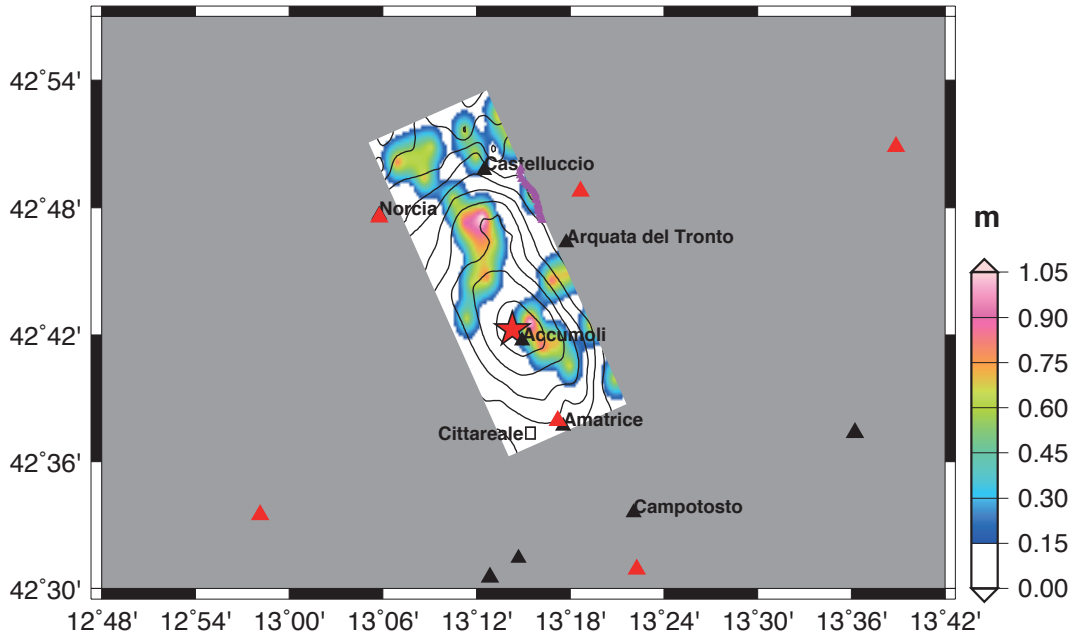

Figure 4. Inverted rupture model projected on the Earth surface with villages up to 20km distant from the nucleation. Colors on the fault plane indicate the slip distribution; black contours represent the position of the propagating rupture at 1 s interval. Violet line displays the location of the observed surface breakages (provided by S. Gori & E. Falcucci-EMERGEO)

References

Cirella, A., A. Piatanesi, E. Tinti, and M. Cocco (2008), Rupture process of the 2007 Niigata-ken Chuetsu-oki earthquake by non-linear joint inversion of Strong Motion and GPS data, *Geophys. Res. Lett.*, *35*, L16306, ISSN: 0094-8276, doi: 10.1029/2008GL034756

Cirella A., Piatanesi A., Tinti E. Chini M. and M. Cocco (2012), "Complexity of the rupture process during the 2009 L'Aquila, Italy, earthquake", *Geophysical Journal International.*190, 607-621, doi:10.1111/j.1365-246X.2012.05505.x.

Piatanesi, A., A. Cirella, P. Spudich, and M. Cocco (2007). A global search inversion for earthquake rupture history: Application to the 2000 western Tottori, Japan earthquake. *J. Geophys. Res.*, *112* (B7), B07314, ISSN: 0148-0227, doi: 10.1029/2006JB004821.

Pulido, N. & Dalguer, L., 2009. Estimation of the high-frequency radiation of the 2000 Tottori (Japan) earthquake based on a dynamic model of fault rupture: application to the strong ground motion simulation, Bull. seism. Soc. Am., 99(4), 2305–2322, doi:10.1785/0120080165. Reale, D., Nitti, D.O., Peduto, D., Nutricato, R., Bovenga, F. & Fornaro.